Optimal Aero-Elastic Design of a Rotor with Bend-Twist Coupling

McWilliam, Michael; Zahle, Frederik; Dicholkar, Antariksh Chandrashekhar; Verelst, David Robert; Kim, Taeseong

Published in:
Journal of Physics: Conference Series

Link to article, DOI:
10.1088/1742-6596/1037/4/042009

Publication date:
2018

Document Version
Publisher's PDF, also known as Version of record

Optimal Aero-Elastic Design of a Rotor with Bend-Twist Coupling

IOP Conf. Series: Journal of Physics: Conf. Series **1037** (2018) 042009 doi:10.1088/1742-6596/1037/4/042009

Optimal Aero-Elastic Design of a Rotor with Bend-Twist Coupling

Michael K. McWilliam[1], Frederik Zahle[1], Antariksh Dicholkar[1], David Verelst[1], Taeseong Kim[1]

[1] Wind Energy Department, Technical University of Denmark, Frederiksborgvej 399, 4000 Roskilde

E-mail: mimc@dtu.dk

Abstract.

Passive Bend-Twist Coupling (BTC) can be used in blades to alleviate loads and generate more Annual Energy Production (AEP). However, BTC is inherently aero-elastic, thus difficult to incorporate into the design with sequential design process. Multi-disciplinary Design Optimization (MDO) is an attractive approach for overcoming these challenges. This paper presents the re-design of a 100kW BTC rotor using the MDO rotor design package HAWTOpt2. In the preliminary design phase, MDO was used to assess the differences between elastic BTC (*i.e.* off-axis fibers) and geometric BTC (*i.e.* sweep). This work found that aero-elastic design optimization without BTC was able to achieve a 16% improvement, then with sweep a 18% improvement and with material coupling a 17% improvement. Due to the reduced stiffness of off-axis fibers, material coupled designs had more difficulty satisfying the tip deflection constraint. The geometric BTC concept was chosen for the final design. The design optimization was repeated with additional manufacturing constraints. The final design achieved a 12% improvement.

1. Introduction

Bend-Twist Coupling (BTC) has been advocated for many years as a means of reducing the loads on a wind turbine and generating more Annual Energy Production (AEP) [1, 2]. The basic idea is to develop blades that will utilize aero-elastic couplings that cause the blade to deform in ways that dampen fluctuating and extreme loads. One of the early techniques involved taking advantage of the material anisotropy inherent in fiber based laminates [1]. Off-axis fibers will cause the blade to twist with flap-wise bending. This technique is typically referred to as material BTC. A second BTC approach uses in-plane sweeping of the planform [2] to achieve a similar aero-elastic coupling. In this approach, it is the swept shape that is introducing the coupling. This technique is typically referred to as geometric BTC.

There have already been many investigations into BTC. Griffin [3] looked at the materials and the details of the structural design to produce conceptual blade designs with material BTC. Capellaro [4] explored the detailed design of material BTC with advanced cross section analysis and aero-elastic models. These studies have found that there is a trade-off between coupling and flap-wise stiffness. Thus, most researchers recommend modest fiber angles.

The research into geometric BTC has followed a similar line of development. Verelst and Larsen [5] performed a parameter study on swept blades using aero-elastic models to evaluate

how it affects loads. Sandia National Laboratories [2] developed a swept blade design in conjunction with the Knight and Carver wind group. The design was built and tested in a laboratory and eventually the rotor was tested in the field.

Much of the research into BTC has focused on the details of the BTC mechanism itself. Researchers have typically performed parameter studies to understand how BTC will affect the design. Optimal rotor design is a collection of interacting constraints and design variables, so a more holistic assessment is needed to evaluate the impact of BTC. One example is given by Bottasso *et al.* [6] who applied multi-level Multi-disciplinary Design Optimization (MDO) framework to investigate material BTC. The MDO approach showed that BTC could reduce pitch actuation and lead to more robust wind turbine designs. Bottasso *et al.* noted that the load reductions achieved with BTC can be used to increase AEP with larger rotors. However, they did not investigate this potential in their work.

This research is similar to the work of Bottasso, where MDO is used to explore the overall impact of BTC on the rotor design. The research will develop an aero-elastically optimum $100kw$ pitch regulated rotor with BTC. The research in this paper has applied the monolithic MDO framework HAWTOpt2 described in section 2. The monolithic approach is able to capture all the couplings between the disciplines so it can actively size the rotor diameter. The first phase of this research developed multiple blade designs to compare both material and geometric BTC blades (section 3). The preliminary design studies looked at the impact of the different BTC and control strategies. The overall goal of this research is to build the blade and test it in the field, so the results of these preliminary studies were used to develop a final design presented here along with the preliminary designs.

2. Aero-structural Design Tool

The HAWTOpt framework is a monolithic optimization framework based on OpenMDAO v1.x [7]. The framework relies on HAWC2 [8] and HAWCStab2 [9] suite of aero-elastic tools to simulate the IEC 61400-1 Ed3 loads on the turbine [10]. A critical component for investigating material BTC is the BECAS cross section tool [11, 12] that is based on a Finite Element Method (FEM) representation that solves all the coupling in the cross section. The optimization was performed with the IPOPT algorithm [13] was used in conjunction with PyOptSparse [14] with Finite Difference (FD) numerical gradients. The overall workflow is shown in extended design structure matrix diagram (XDSM) [15] in figure 1. Another critical component of the framework is the monolithic structure where the optimization can evaluate the full aero-elastic response of the BTC effects. For more details see Zahle *et al.* [16].

2.1. Blade Parameterization

The blade planform is described in terms of distributions of chord, twist, relative thickness and pitch axis aft leading edge, the latter being the distance between the leading edge and the blade axis. The lofted shape of the blade is generated based on interpolation of a family of airfoils with different relative thicknesses.

The internal structure is defined from a number of regions that each cover a fraction of the cross-sections along the blade. Each region consists of a number of materials that are placed according to a certain stacking sequence. Figure 2 shows a cross section in which the region division points (DPs) are indicated along with the parameterized quantities used to construct the structural geometry. The material layup for a region on the suction side is the same as on the corresponding mirrored region on the pressure side of the cross-section. So for example, Region 1 on the pressure side between the division points DP01 and DP02 has the same laminate layup as Region 14 on the suction side between the points DP15 and DP16. The composite layup is described by a series of smooth splines describing the thicknesses of individual layers. Fore more details on the parameterization see [17].

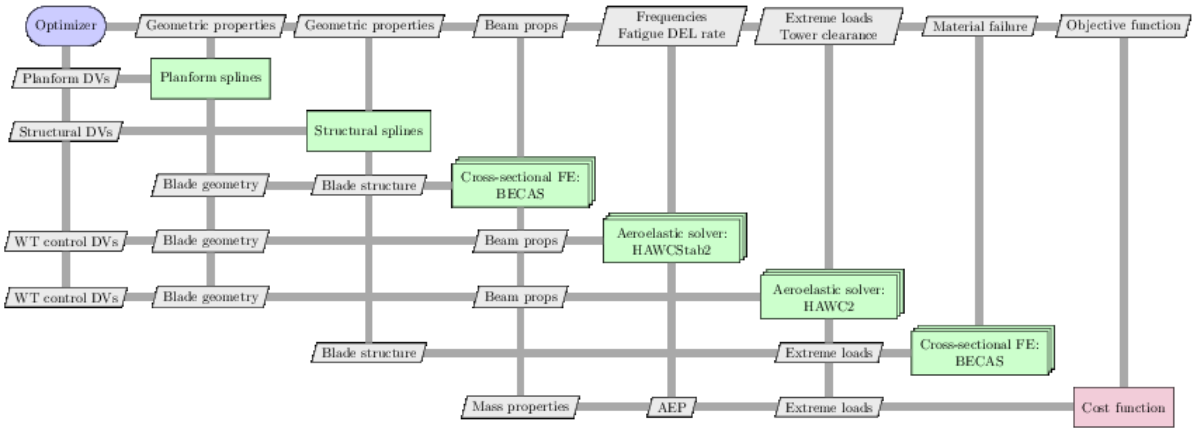

Figure 1: Extended Design Structure Matrix diagram of the work-flow of HAWTOpt2.

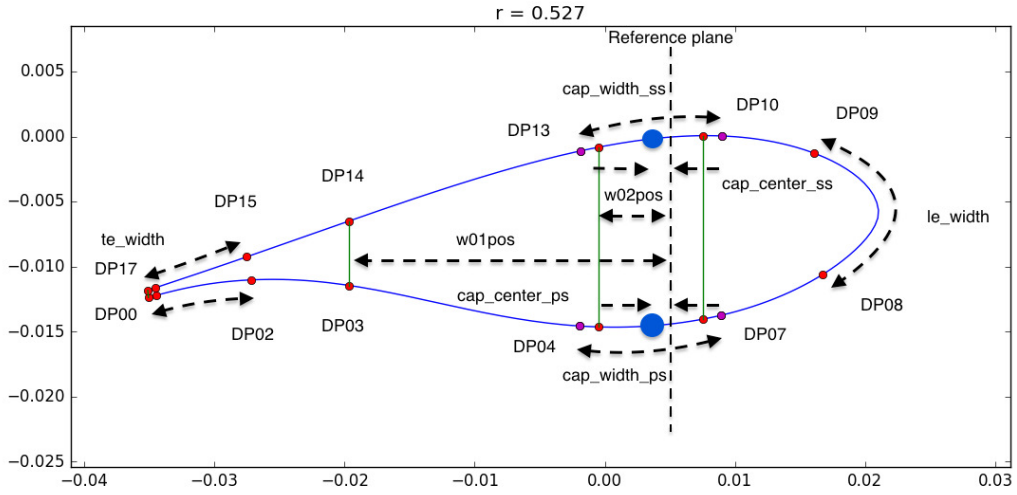

Figure 2: Region division points (DP) definition: red points indicate division points between regions; their positions are defined as curve fraction from pressure side TE (s=-1) to LE (s=0) to suction side TE (s=1).

2.2. Optimization Problem

The optimization is based on solving the problem given in (1). The optimization is essentially a maximization of AEP without increasing the loads on the platform. This is a common industrial design problem where a manufacturer wants to develop a new set of blades for a platform already in existence.

Table 1: Summary of Typical Design Variables

Parameter	# of DVs	**Comment**
Chord	6	-
Twist	5	Root twist fixed
Relative thickness	4	Root and tip relative thickness fixed
Blade prebend	4	-
Pitch axis	4	Lateral position of the cross section
Blade length	1	-
Tip-speed ratio	1	-
Trailing edge Unix	4	Pressure/suction side
Trailing panel Triax	4	Pressure/suction side
Spar cap Uniax	4	Pressure/suction side
Leading panel Triax	4	Pressure/suction side
Leading edge Uniax	4	Pressure/suction side
Spar cap width	4	Width of the spar-cap
Sweep	3	Used only in swept designs
Spar cap Uniax angle	8	Used only in material coupled designs
Total	49-57	

$$\begin{aligned} \underset{\mathbf{x}_p, \mathbf{x}_s, \mathbf{x}_{oper}}{\text{minimize}} \quad & f(\{\mathbf{x}_p,\, \mathbf{x}_s\, \mathbf{x}_{oper}, \mathbf{p}, w) \\ \text{subject to} \quad & \mathbf{g}(\mathbf{x}_p) \leq \mathbf{0}, \\ & \mathbf{h_g}(\mathbf{x}_s) \leq \mathbf{0}, \\ & \mathbf{h_s}(\mathbf{x}_s) \leq \mathbf{0}, \\ & \mathbf{k}(\{\mathbf{x}_p,\, \mathbf{x}_s\}) \leq \mathbf{0} \end{aligned} \tag{1}$$

Where:

$$f(\{\mathbf{x}_p,\, \mathbf{x}_s,\, \mathbf{x}_{oper}\}, \mathbf{p}) \quad = \quad \frac{AEP(\{\mathbf{0},\, \mathbf{0},\, \mathbf{0}\}, \mathbf{p})}{AEP(\{\mathbf{x}_p,\, \mathbf{x}_s,\, \mathbf{x}_{oper}\}, \mathbf{p})} \tag{2}$$

The design variables used in this optimization are shown in table 1. They include a mix of planform, internal structure and control design variables. The critical design variable is the blade length. Load reduction strategies are used to allow the rotor to increase in size without increasing the total loads.

The constraints used in the problem are shown in table 2.

3. Design Studies

The initial design is loosely based on a $100kw$ commercial design by Hummer [18]. The original planform and aero-elastic properties were used to develop a fully described initial design. The FFA-W airfoil series was selected, with the NACA 63-418 airfoil used at the tip. The airfoil polars were generated with Computational Fluid Dynamics (CFD) with a Reynolds number of 10^6, which is representative of the average conditions of this turbine under normal operation. The internal structure design was based on the same box-spar topology and glass fiber materials as the DTU 10MW Reference Wind Turbine Design (RWT) [19]. An inverse blade design, based on the known structural properties, was conducted to determine the initial material distributions throughout the blade. The predicted loads of this turbine were used as the reference values in the design constraints.

Table 2: Summary of Optimization Constraints

Constraint	Value	**Comment**
max(chord)	< 1.02 m	Maximum chord limited for transport.
max(prebend)	< 1.02 m	Maximum prebend limited for transport.
min(relative thickness)	> 0.18	Same airfoil series as used on the DTU 10MW RWT.
min(material thickness)	> 0.0	Ensure FFD splines do not produce negative thickness.
$t/w_{sparcap}$	> 0.08	Basic constraint to avoid spar cap buckling.
min(tip tower distance)	$>$ ref value	DLC1.3 operational tip deflection cannot exceed that of the DTU 10MW RWT.
Steady state rotor thrust	< 1.07 ref value	Steady state solution for steady uniform inflow
Steady state root flap-wise moment	< 1.07 ref value	Steady state solution for steady uniform inflow
Blade root flap-wise moments (MxBR)	$<$ ref value	DLB loads cannot exceed starting point.
Blade root edgewise moments (MyBR)	$<$ ref value	DLB loads cannot exceed starting point.
Blade root edgewise moments (MzBR)	$<$ ref value	DLB loads cannot exceed starting point.
Tower top thrust (FyTT)	$<$ ref value	DLB loads cannot exceed that starting point.
Tower bottom fore-aft moments (MxTB)	$<$ ref value	DLB loads cannot exceed that starting point.
Rotor torque	$<$ ref value	Ensure that the rotational speed is high enough below rated to not exceed generator maximum torque.
Blade mass	< 1.05 * ref value	Limit increase in blade mass to maintain equivalent production costs.
Blade mass moment	< 1.05 * ref value	Limit increase in blade mass moment to minimize edgewise fatigue.
Lift coefficient @ $r/R = [0.5 - 1.]$	< 1.16	Limit operational lift coefficient to avoid stall for turbulent inflow conditions.
Ultimate strain criteria	< 0.9	Aggregated material failure in each section for all load cases.

In the first phase of the project, three different design optimizations were performed to evaluate the most appropriate form of BTC to be used in the final design. The difference between each of the optimal designs was the BTC design variables that were included in the optimization. In the first (referred to as KB1), has no sweep or material coupling and shows the improvement from aero-elastic design optimization alone. The second design (KB2) optimized the same design variables as KB2 and allowed the blade to sweep at the tip. Similarly, the third design (KB3) optimized the same design variables as KB1, but allowed the optimization to vary the fiber angle.

The preliminary design studies showed that the swept blade showed the greatest potential, so all subsequent design optimizations looked at rotor sweep. In the fourth design optimization (KB4) several additional manufacturing constraints were imposed on the design. Furthermore, to simplify the controller design, the optimization was not allowed to change the tip-speed-ratio in the KB4 optimization. The KB4 demonstrated the importance of varying the tip-speed-ratio in the design optimization. A final design (KB5) was developed with many of the same design variables and constraints as KB4. In KB5 the optimization was able to vary the tip-speed-ratio as well.

A summary of the different designs is described below.

- **KB1**: Optimized straight blade. This blade is optimized with constraints on blade torsion to be less than 1 degree at the tip, and no design freedom is given to introduce sweep or material couplings.
- **KB2**: Optimized swept blade. This blade is optimized without constraints on blade torsion and given design freedom to introduce sweep, but not material couplings.
- **KB3**: Optimized material coupled blade. This blade is optimized without constraints on blade torsion and given design freedom to introduce material couplings in the spar cap, but not sweep.
- **KB4**: Optimized swept blade with fixed rotor speed schedule. This blade is optimized without constraints on blade torsion and given design freedom to introduce sweep, but not material couplings. Compared to KB2, additional constraints have been placed on the sweep and prebend. The sweep is constrained to achieve only backward sweep with a maximum limit on its value not exceeding 5% of the reference blade length. The sweep is only allowed from 60% blade span and onwards. The prebend too has been constrained to only bend away from the tower with a maximum limit on its value not exceeding 10% of the reference blade length. An outer layer of Triax is added, which is maintained at a fixed thickness through the optimization. The spar cap width is disallowed design freedom. These design decisions have been taken to address manufacturing and structural concerns. Importantly, this design has a fixed rotor speed schedule calculated based on the design tip-speed ratio of the reference blade.
- **KB5**: Optimized swept blade. This blade is optimized without constraints on blade torsion and given design freedom to introduce sweep, but not material couplings. It incorporates the same design decisions as applied to KB4. However, unlike KB4 the rotor speed schedule is allowed design freedom to vary through the optimization.

3.1. Optimal Performance

A summary of the optimal designs is given in table 3. The optimization of the KB1, KB2 and KB3 designs were based on a Weibull distribution with a scale of 6 and a shape of 2. While the KB4 and KB5 designs were based on a Weibull distribution with a scale of 6 and a shape of 2. The AEP for both wind distributions is presented for all the designs. Looking at the KB1 design, the aero-elastic optimization alone improved the AEP by 14.8%. KB2 shows that sweep can improve the AEP by an additional 3.94%, while optimization with material coupling only

added an addition 2.48%. Closer inspection showed that the material coupled design was limited by the tip deflection constraint. This confirms that the reduced flap-wise stiffness from biased fibers limits the extent that material coupling can be utilized in a rotor design.

Table 3: Summary of overall properties of the five optimized blades.

Quantity	Reference	KB1		KB2		KB3		KB4		KB5	
	Value	Value	Change	Value	Change	Value	Change	Value	Change	Value	Change
AEP[MWhr] (A=6, k=2)	212.38	243.82	+14.80%	252.18	+18.74%	249.08	+17.28%	224.67	+5.79%	236.77	+11.48%
AEP[MWhr] (A=9.59, k=2)	487.14	521.92	+7.14%	529.33	+8.66%	528.45	+8.48%	501.19	+2.88%	514.60	+5.64%
Blade length [m]	10	11.06	+10.6%	11.41	+14.1%	11.22	+12.2%	10.48	+4.8%	10.55	+5.5%
Blade mass [kg]	273.16	256.87	-5.96%	257.71	-5.66%	256.65	-6.04%	254.53	-6.82%	260.46	-4.65%
TSR [-]	7.50	10.08	+34.4%	10.62	+41.67%	9.78	+30.39%	7.68	+2.4%	9.77	+30.27%

Figure 3 shows that the power improvement comes from the below rated conditions. There is a discrepancy in the above rated power for the KB3 design because the power curve was evaluated with different tools. The reader should assume the actual above rated performance is the same for all the designs.

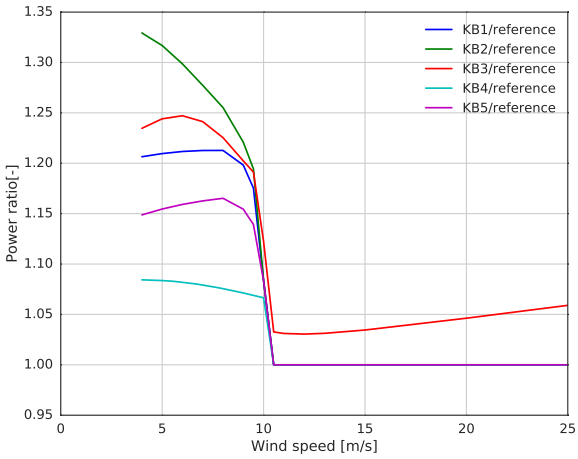

Figure 3: Ratio of mechanical power as function of wind speed for the optimized blades relative to the reference.

Figure 4 shows the coefficient of power and thrust for all the blades. All the optimal designs except for the KB5 design, all had lower C_P than the reference design. This shows that the optimization is choosing less efficient designs because the reduced loads allow the design to increase the production through larger rotors. In the KB5 design the optimization increased the rotor radius and the coefficient of power simultaneously. Since the final design was based on this optimization, additional optimizations were performed to ensure that the optimization was fully converged. The downward trends in the C_T shows that the optimization is using the BTC to reduce the peak loads that occur near rated conditions.

3.2. Optimal Designs

Figure 5 shows the optimal plan-forms for the different designs. Overall the optimization selected lower-solidity designs. This would lead to reduced tower clearance, so the optimization increased the pre-bend and relative thickness to compensate. The BTC designs had a more aggressive twist distribution to compensate for the torsional deformation.

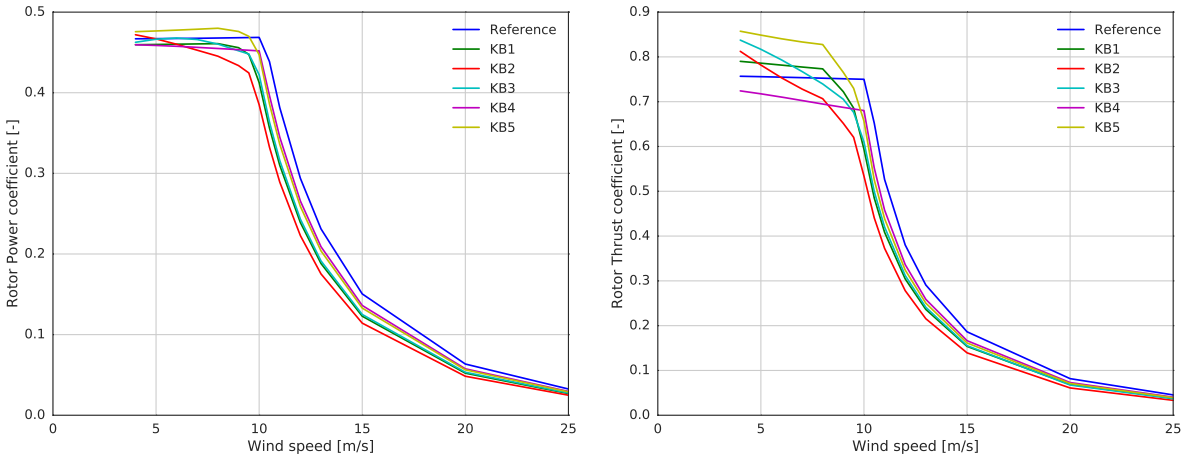

(a) C_P (b) C_T

Figure 4: Mechanical power and thrust coefficient as function of wind speed for the five optimized blades.

Figure 6 shows that the optimization is increasing the spar-cap thickness at the root while reducing the thickness towards the tip. Overall the optimization focused most on changing the thickness of the Uniax material and only slightly increased the thickness of the Triax. The optimization chose to increase the spar-cap width by approximately 5%. The optimization was allowed to vary the thickness in other regions of the blade, but no significant changes were seen in these regions.

Figure 7 shows the sweep in all the designs, along with the fiber angle that was selected in the KB3 design. In all the swept designs, the optimization chose the largest sweep it was allowed. The optimization was allowed to vary the sweep for the full span in the KB2, however only chose significant sweep in the outer 20% of the blade. The sweep in the KB4 and KB5 design was not allowed to start until 60% of the radius, however the KB2 results indicate that relaxing this constraint would have had little impact on the outcome.

In the KB3 design, the fiber angle parameterization was simplified by using continuously varying splines, for both the pressure and suction side of the spar cap. This is not realistic for manufacturing reasons, however the intention was the initial phase was for design exploration and that manufacturing constraints would only be considered for the final design. The results indicate that the optimization prefers modest biased fibers (7.5°) towards the tip and more on the suction side of the blade. This is well within the fiber angle constraints imposed on the optimization, so it appears that the optimization could not include more coupling without violating other constraints (*i.e.* tip deflection).

The results of the preliminary designs showed that swept design had greater potential in improving the AEP. The next phase of the project focused on developing a blade design that could be manufactured. This involved constraining the amount of sweep, the curvature and the minimum material thickness in the blade. In all the preliminary designs, the optimization selected high tip-speed operation in the variable speed region. There was a concern that this would be problematic for the platform so the first optimization constrained the rotor speed schedule to be the same as the original design. However, the results show this over-constrained the design and limited the extent that sweep could be used to improve the AEP. So this constraint was relaxed for the final design which led to the final design shown in figure 8.

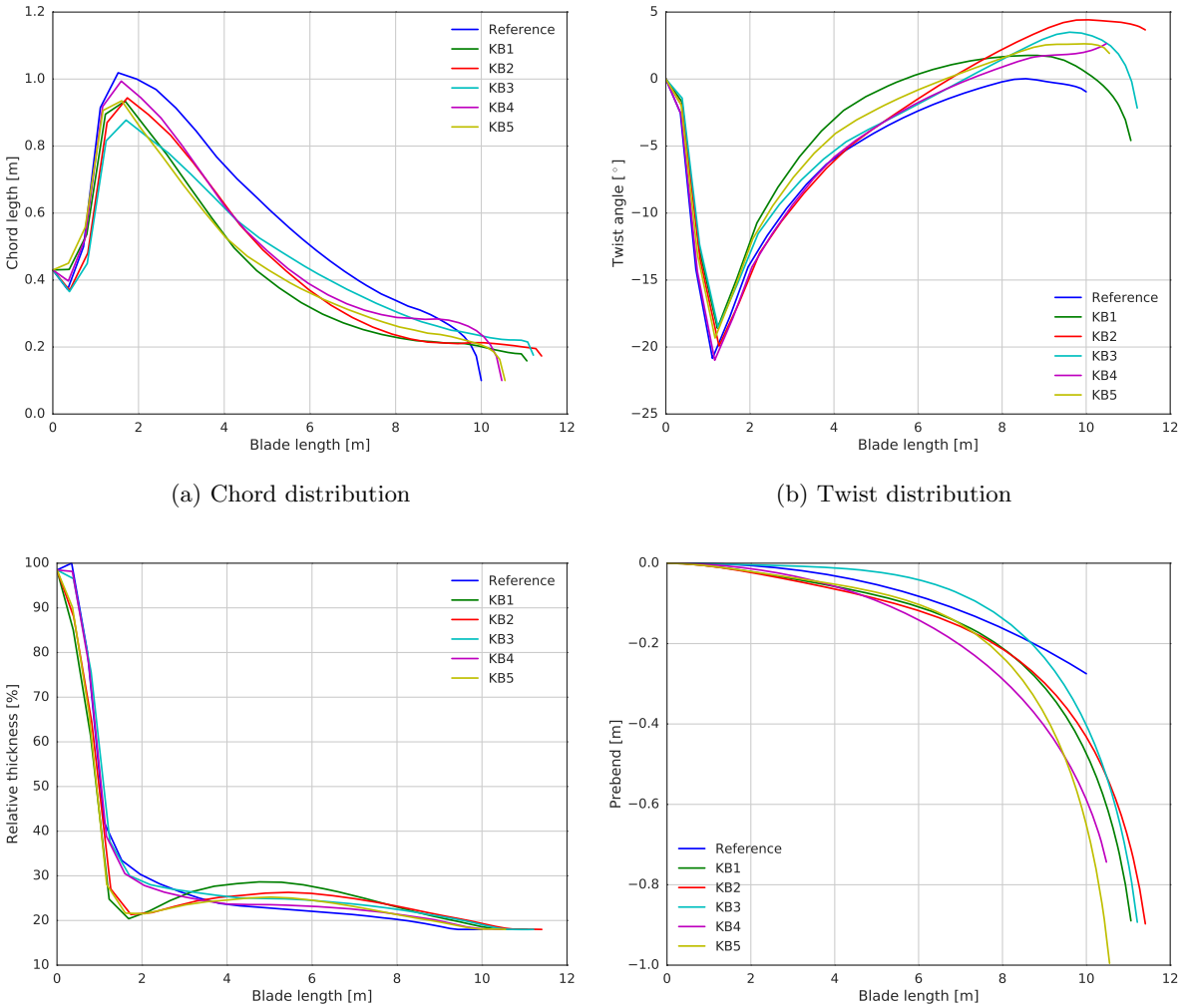

(a) Chord distribution

(b) Twist distribution

(c) Relative thickness distribution

(d) Pre-bend

Figure 5: Blade planform properties

3.3. Optimization Convergence

Figure 9 shows the evolution of the KB5 optimization along with the normalized constraints. The optimization was allowed to run for a significant number of iterations. After 175 iterations it is clear that the optimization is not able to make any more progress. The optimization relies on finite difference gradients which contain some error. After a certain point in the optimization, this error dominates the optimization and the algorithms cannot accurately solve the design variations that will improve the design. The relatively flat objective values and the frequent constraint violations near the end of the optimization indicate that the optimization had reached this point. The best feasible solution was chosen as the final design.

Figure 9b shows that many of the constraints were active or close to active for the best feasible solution. This confirms that the optimization had little room to further improve the design. The constraints show that the design is driven by the torque constraint with is defined by the power rating, the steady state flap-wise bending moment, tip deflection, pre-bend, sweep, blade failure,

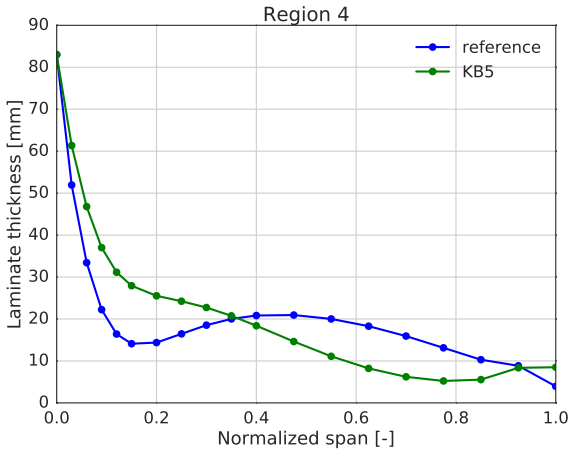

Figure 6: Spar-cap laminate thickness in comparison with reference

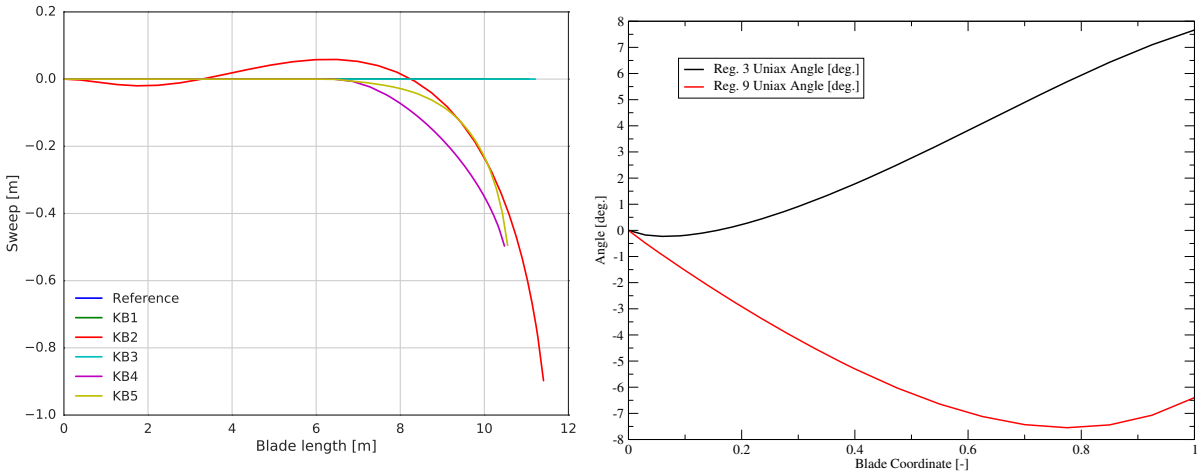

(a) Sweep (b) Fiber Angle

Figure 7: Blade sweep and fiber angle

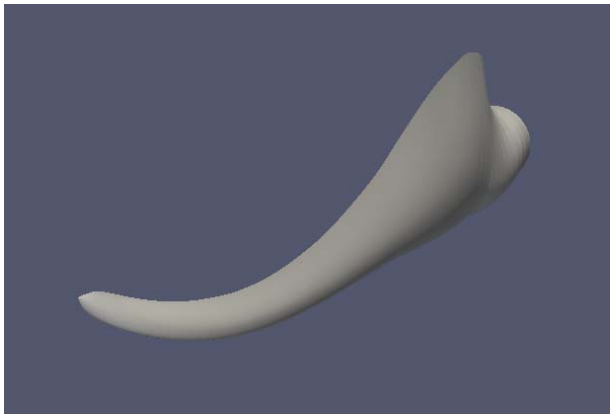

Figure 8: Visualization of the final KB5 design

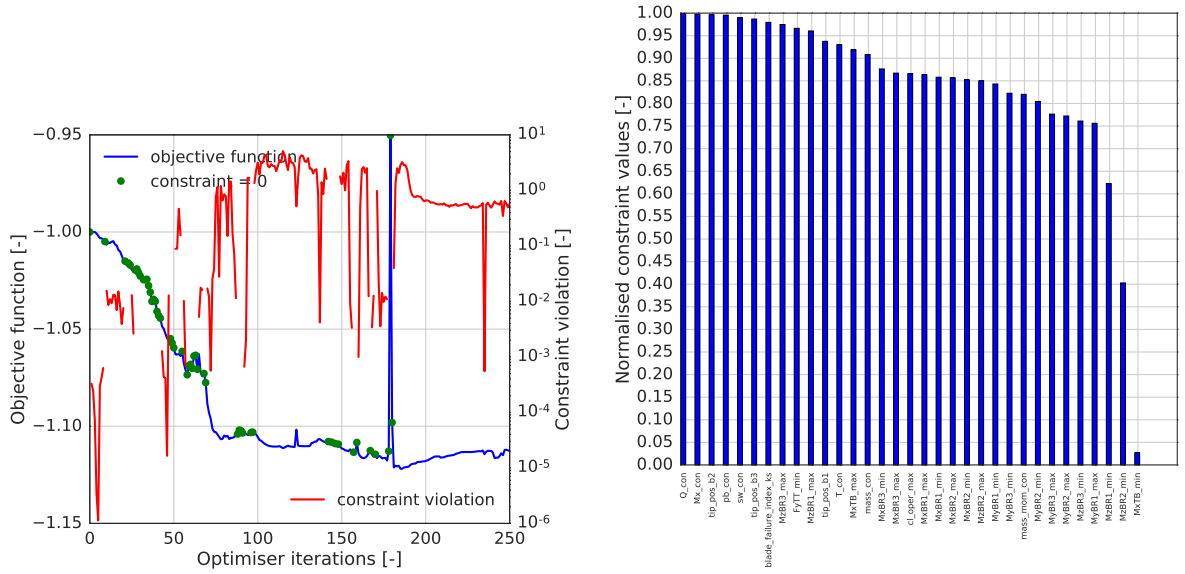

(a) Optimization evolution (b) Normalized constraints

Figure 9: The evolution of the optimization and the driving constraints

blade torsion loads and tower top thrust. The fact that a variety of unrelated constraints are active shows the optimization has taken advantage of all the design freedom available.

3.4. Full design load basis

The final KB5 design was evaluated in HAWC2 with a full Design Load Basis (DLB) and compared with the DLB of the reference design. Overall, the KB5 rotor had similar similar loads as the reference in nearly all simulation and all sensors. However, the swept blade generates more torsion and this can be seen in figure 10. This indicates that overall the same platform can accommodate this design, however, the hub connection and the pitch actuator may need to be reinforced to hold the increased torsion loading.

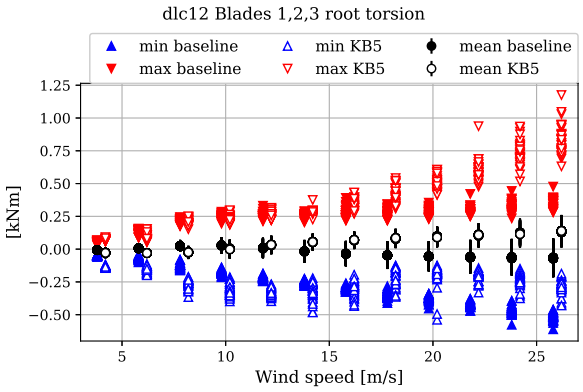

Figure 10: Blade root 1, 2 and 3 torsion bending moments [kNm] (pitching coordinates)

4. Conclusions

This paper presents the design of a $100kW$ BTC blade with a monolithic MDO framework. Overall, the optimization was able to increase the AEP by increasing the size of the rotor. This is enabled by using BTC to reduce the peak loads near rated conditions.

In the first phase, manufacturing constraints were ignored to explore the best BTC strategy. The optimization showed that swept blades showed the greatest potential. With material coupling, the design must reduce the flap-wise stiffness to increase the coupling. This trade-off is not present in the swept design so the optimization is able to achieve greater coupling. Overall, the optimization showed that sweep is 59% more effective in increasing the AEP than material coupling.

A second round of design optimization was conducted with additional manufacturing constraints. In the second round the blade could not achieve the same improvements because the sweep magnitude was constrained. At the final solution, multiple unrelated constraints were active, showing there was little room to further improve the design. This final design was evaluated with a full DLB. This analysis showed that the final design produced the same loads as the original design except in blade root torsion. The increased blade root torsion is a direct result of the blade sweep, thus a reinforced root connection, pitch bearing and pitch actuator is required.

References

[1] Don W. Lobitz and Paul S. Veers. Aeroelastic Behavior of Twist-Coupled HAWT Blades. In *1999 ASME Wind Energy Symposium*, January 1999.

[2] Tom Ashwill. Sweep-Twist Adaptive Rotor Blade: Final Project Report. Technical report, Knight & Carver Wind Group and Sandia National Laboratories, 2423 Hoover Avenue National City, California 91950 and PO Box 5800 Albuquerque New Mexico 87185 and Livermore California 94550, February 2010. SAND2009-8037.

[3] Dayton A. Griffin. Evaluation of Design Concepts for Adaptive Wind Turbine Blades. Technical report, Sandia National Laboratory, Albuquerque, New Mexico, August 2002. SAND2002-2424.

[4] Mark Capellaro. Design Limits of Bend Twist Coupled Wind Turbine Blades. In *53rd AIAA Structures, Structural Dynamics and Materials Conference, April 23-26 2012, Honolulu Hawaii*, April 2012.

[5] David Robert Verelst and Torben J. Larsen. Load consequences when sweeping blades – a case study of a 5 mw pitch controlled wind turbine. Technical report, Technical University of Denmark, 2010.

[6] C.L. Bottasso, F. Campagnolo, A. Croce, and C. Tibaldi. Optimization-based study of bend-twist coupled rotor blades for passive and integrated passive/active load alleviation. *Wind Energy*, 2011.

[7] Justin Gray, Kenneth T. Moore, Tristan A. Hearn, and Bret A. Naylor. Standard platform for benchmarking multidisciplinary design analysis and optimization architectures. *AIAA Journal*, 51(10):2380–2394, Oct 2013.

[8] Torben Juul Larsen and Anders Melchoir Hansen. How 2 hawc2, the user's manual. Manual, Ris, July 2015.

[9] M. H. Hansen. Aeroelastic Stability Analysis of Wind Turbines Using an Eigenvalue Approach. *Wind Energy*, 7:133–143, 2004.

[10] Morten Hartvig Hansen, Kenneth Thomsen, Anand Natarajan, and Thanasis K. Barlas. Design load basis for onshore turbines - revision 00. Technical report, Danish Technical University, 2015.

[11] Jos Pedro Blasques and Mathias Stolpe. Multi-material topology optimization of laminated composite beam cross sections. *Composite Structures*, 94(11):3278 – 3289, 2012.

[12] DTU. Beam cross section analysis software. http://www.becas.dtu.dk/, 2018.

[13] Andreas Wächter and Lorenz T. Biegler. On the implementation of an interior-point filter line-search algorithm for large-scale nonlinear programming. *Mathematical Programming*, 106(1):25–57, Mar 2006.

[14] Pyopt. http://www.pyopt.org/, 2018.

[15] Andrew Lambe and Joaquim Martins. Extensions to the design structure matrix for the description of multidisciplinary design, analysis, and optimization processes. *Structural and Multidisciplinary Optimization*, 46(2):273–284, 2012.

[16] Frederik Zahle, Carlo Tibaldi, Christian Pavese, Michael McWilliam, Jose Pedro Albergaria Amaral Blasques, and Morten H. Hansen. Design of an aeroelastically tailored 10 mw wind turbine rotor. *Journal of Physics: Conference Series*, 753, October 2016.

[17] Pierre-Elouan Rethore, Frederik Zahle, Katherine Dykes, Peter Graf, and Andrew Ning. Framework for unified systems engineering and design of wind plants, 2018.

[18] Hummer. Hummer 100kw wind turbine, http://www.chinahummer.cn/index.php/index/content/111, 2016.
[19] Christian Bak, Frederik Zahle, Robert Bitsche, Taeseong Kim, Anders Yde, Lars Christian Henriksen, Anand Natarajan, and Morten Hartvig Hansen. Description of the dtu 10 mw reference wind turbine. Technical report, Technical University of Denmark Institute for Wind Energy, 2013.